

September 01, 1992

## Positron two-dimensional angular-correlation-of-annihilation-radiation study of untwinned $\text{YBa}_2\text{Cu}_3\text{O}_{6.9}$ in the a-axis projection

L. C. Smedskjaer

*Argonne National Laboratory*

A. Bansil

*Northeastern University*

U. Welp

*Argonne National Laboratory*

Y. Fang

*Argonne National Laboratory*

K. G. Bailey

*Argonne National Laboratory*

---

### Recommended Citation

Smedskjaer, L. C.; Bansil, A.; Welp, U.; Fang, Y.; and Bailey, K. G., "Positron two-dimensional angular-correlation-of-annihilation-radiation study of untwinned  $\text{YBa}_2\text{Cu}_3\text{O}_{6.9}$  in the a-axis projection" (1992). *Physics Faculty Publications*. Paper 416.

## Positron two-dimensional angular-correlation-of-annihilation-radiation study of untwinned $\text{YBa}_2\text{Cu}_3\text{O}_{6.9}$ in the $a$ -axis projection

L. C. Smedskjaer

*Materials Science Division, Argonne National Laboratory, Argonne, Illinois 60439*

A. Bansil

*Physics Department, Northeastern University, Boston, Massachusetts 02115*

U. Welp, Y. Fang, and K. G. Bailey

*Materials Science Division, Argonne National Laboratory, Argonne, Illinois 60439*

(Received 7 May 1992)

We present a two-dimensional (2D)-ACAR positron annihilation study of an *untwinned*  $\text{YBa}_2\text{Cu}_3\text{O}_{6.9}$  metallic sample in the  $a$ -axis projection; all existing data from untwinned samples have employed the  $c$  projection. The data show a clear presence of the Cu-O chain related ridge Fermi surface extending along the  $\Gamma Z$  direction and two associated umklapp images at higher momenta. These results are consistent with the previously investigated  $c$  projection of the momentum density in  $\text{YBa}_2\text{Cu}_3\text{O}_{6.9}$  and do not appear to indicate a strong localization of these electron states along the  $c$  direction. We compare and contrast the structures in 2D-ACAR's in the  $a$  and  $c$  projections, delineating similarities and differences between the results for the two projections.

### I. INTRODUCTION

The two-dimensional angular correlation of annihilation radiation (2D-ACAR) experiment constitutes a powerful spectroscopy of the electronic structure of materials. 2D-ACAR studies of  $\text{YBa}_2\text{Cu}_3\text{O}_{7-x}$  were started immediately after its discovery to explore the Fermiology of the new superconductors. The pioneering work on twinned specimens<sup>1-3</sup> led to investigations of *untwinned* samples. These latest experiments<sup>4-7</sup> involving the  $c$  projection, in conjunction with corresponding calculations of the 2D-ACAR spectral intensities based on the conventional band theory framework, have shown clear signatures of the Cu-O chain-related ridge Fermi surface (FS), as well as indications of the smaller "pillbox" FS around the  $S$ -symmetry point, all in remarkable agreement with theoretical predictions. The Cu-O chain FS has so far not been identified clearly by other relevant spectroscopies, and thus the 2D-ACAR experiment has played a crucial role in piecing together the overall fermiology of  $\text{YBa}_2\text{Cu}_3\text{O}_7$ .<sup>8</sup> Although  $\text{YBa}_2\text{Cu}_3\text{O}_{7-x}$  has been the most extensively investigated superconductor, 2D-ACAR work has been reported for  $\text{Bi}_2\text{Sr}_2\text{CaCu}_2\text{O}_{8+x}$ ,<sup>9,10</sup> and  $\text{La}_{2-x}\text{Sr}_x\text{CuO}_4$ .<sup>11,12</sup>

In this paper, we investigate the fermiology of  $\text{YBa}_2\text{Cu}_3\text{O}_7$  in the  $a$ -axis projection; similar measurements are in progress elsewhere.<sup>13</sup> As noted, all existing measurements for *untwinned* samples are in the  $c$  projection. A number of measurements with projections in the  $a$ - $b$  plane have, however, been published for *twinned* specimens, but do not report the observation of Cu-O chain related bands.<sup>1</sup> As in the case of the  $c$  projection, here also the use of the *untwinned* specimen is important for clearly delineating structure in the momentum density.

The present  $a$  projection provides another picture of the momentum density of the untwinned material. Further, some current theoretical views hold that there may be fundamental differences in the description of the electron states (e.g., localized vs itinerant) in the  $a$  or  $b$  directions compared to the  $c$  direction.<sup>14</sup> In this regard, because an  $a$  projection does not involve a momentum-density integration in the  $c$  direction, it is more sensitive to the electronic wave function character along the  $c$  direction than is the  $c$  projection. Also, since the  $c$ -projected momentum densities in  $\text{YBa}_2\text{Cu}_3\text{O}_7$  are in striking agreement with band-theory predictions,<sup>15-20</sup> it would be interesting to establish whether the band theory continues to provide a reasonable description of the  $a$ -projected spectra.

### II. RESULTS AND DISCUSSION

The sample was the same *untwinned* single crystal of  $\text{YBa}_2\text{Cu}_3\text{O}_{6.9}$ , displaying a transition at 91 K (width 1 K), as used in Ref. 6 for  $c$  projections, and the present measurements were done under similar conditions. The spectrum, with  $53 \times 10^6$  counts, was found to possess  $C_{2v}$  symmetry after efficiency correction, and to augment statistics the data were symmetrized accordingly.<sup>21</sup> The measurements were carried out at 300 K, and the resolution [full width at half maximum (FWHM)] of the instrument, taking both the finite sample size and the broadening due to thermal motion into account, is 0.7 mrad.

The as-observed 2D-ACAR spectrum appears quite featureless, as expected. Following common practice, the structure in the data may be exposed by considering the *anisotropic* distribution

$$A(\mathbf{p}) = M(\mathbf{p}) - S(\mathbf{p}) \quad (1)$$

where  $M(\mathbf{p})$  denotes the as observed data, and  $S(p)$  is a smooth isotropic function. The resulting data  $A(\mathbf{p})$  will depend somewhat on the choice of  $S(p)$ ; the structures in  $A(\mathbf{p})$  are, however, to a large degree insensitive to  $S(p)$ .

To characterize the present  $a$ -axis data, we recall the nature of the  $c$ -projected 2D-ACAR first; see Fig. 1 (right frame). The major features of the  $c$  projection are the “ridge” running along the crystal  $a$  direction (or equivalently the  $\Gamma X$  direction), four “mountains” that surround the ridge, located along  $\Gamma S$ , and less prominent “side ridges” parallel to the central ridge at a distance of about 13 mrad. The central ridge and the side ridges can be shown to possess  $C_{2v}$  (fourfold) symmetry and to arise mainly from the Cu-O chains and the associated ridge Fermi surface (FS). The mountains, on the other hand, possess  $C_{4v}$  (eightfold) symmetry and may contain contributions from both Cu-O planes and the chains.<sup>5,6,15–20</sup>

The major features of the  $a$  projection are seen from Fig. 1 (left frame) to be, the central ridge extending along the  $c$  direction (i.e., the  $\Gamma Z$  direction), a clear image of the ridge at a distance of about 6 mrad, and a weaker image around 13 mrad. [For orientation, the Brillouin zone (BZ) in  $\text{YBa}_2\text{Cu}_3\text{O}_7$  is in the shape of a slab of approximate dimensions  $6.3 \times 6.3 \times 2.1$  mrad<sup>3</sup>.] These results are consistent with those for the  $c$  projection in that they are dominated by the Cu-O chain states and the related electron ridge FS stretching along the  $a$  direction. In the present  $a$  projection, the spectra would then be expected to show the central ridgeline feature and its images along the  $b$  direction separated by multiples of the BZ dimension, as observed.

Figure 1 allows us to delineate similarities and differences between the signature of the Cu-O chain as revealed by the central ridge and its umklapp images in the two projections. The central ridge in both projections contains a minimum at  $p=0$  and two peaks around  $\pm 5$  mrad, but in the  $a$  projection the anisotropic distribution extends to higher momenta and possesses additional peaks at  $\pm 10$  mrad. The 6-mrad first umklapp image of the ridge in the  $\Gamma Y$  direction is clearer in the  $a$  projection (ridge parallel to  $\Gamma Z$ ); although hidden in the perspective view, this image is present also in the  $c$  projection (ridge parallel to  $\Gamma X$ ), but the mountains overlap with this feature, reducing the momentum range over which it can be observed. Finally, the second umklapp image of the

ridge around 13 mrad is seen in both projections. That the central ridge in both projections displays similar undulations in the  $\Gamma Z$  and  $\Gamma X$  directions may at first sight appear surprising because in the  $a$  projection the ridge extends along the  $c$  direction, while in the  $c$  projection it extends along the  $a$  direction, and the BZ dimensions in the  $c$  and  $a$  directions are widely different. This insensitivity of the momentum density to the tripling of the unit cell in the  $c$  direction indicates that the electron wave functions approximately behave as if the lattice dimension in the  $c$  direction were  $\frac{1}{3}$  of the real lattice distance. This does not constitute a violation of the Bloch theorem, since any function with a period of  $\frac{1}{3}$  of a lattice distance obviously also possesses a period of 1 lattice distance. The results of Fig. 1 are consistent with a picture where no dramatic change (e.g., itinerant vs localized) takes place in the nature of the Cu-O chain wave functions between the  $a$  and  $c$  directions. In particular, our results suggest that these electronic states are not strongly localized along the  $c$  direction.

The mountains seen in the  $c$  projection of Fig. 1 are conspicuously absent in the  $a$  projection. The reason appears to be that on the low-momentum side the mountains contain a dip (hidden from view in the perspective of Fig. 1), which upon performance of an  $a$  integration will tend to compensate the contribution of the peaks.

Further insight into the data is provided by Fig. 2, which shows sections along the  $\Gamma Y$  direction through the spectra of Fig. 1. Some of the points brought out in connection with Fig. 1 above are also evident here. For example, in both projections, as one moves towards the right, starting with  $p=0$ , a steep drop is encountered, which in view of the detailed analysis of the  $c$  projection can be associated with the ridge FS. This is followed by the peaks around 6 and 12 mrad, whose right-hand sides correspond to the first and the second umklapp images of the ridge FS, respectively.

Figure 2 shows that the amplitude of the anisotropy (defined as the difference between the maximum and minimum values—note scales) is roughly two times larger for the  $c$  projection compared to the  $a$  projection; a similar conclusion is reached if differences between sections along pairs of directions (e.g.,  $\Gamma Y$ - $\Gamma Z$ ) are considered.

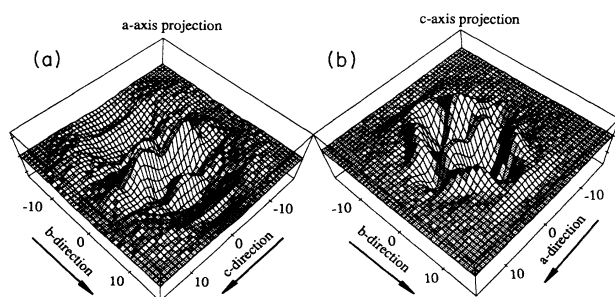


FIG. 1. A three-dimensional rendition of the anisotropic spectra  $A(\mathbf{p})$ , see Eq. (1), for untwinned  $\text{YBa}_2\text{Cu}_3\text{O}_{6.9}$ . (a) The present  $a$  projection, and (b) the  $c$  projection from the data of Ref. 5. The pixel size is  $0.8 \times 0.8$  mrad<sup>2</sup>.

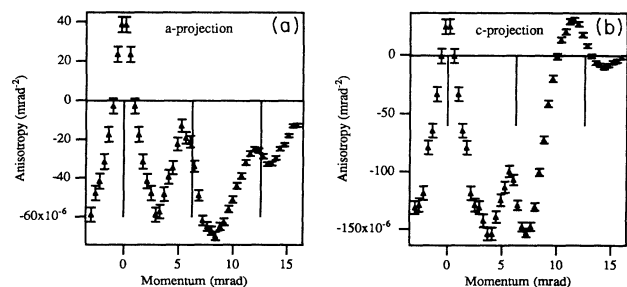


FIG. 2. Sections along  $\Gamma Y$  (the crystal  $b$  axis) through the anisotropic distributions of Fig. 1. The horizontal scale gives  $p_y$ , with the zero corresponding to the  $\Gamma$  point. (a) The  $a$  projection, data integrated over 3 mrad in the  $c$  direction, and (b) the  $c$  projection, data integrated over 0.8 mrad in the  $a$  direction. The solid vertical lines are separated by the reciprocal lattice vector (6.3 mrad) along the  $\Gamma Y$  direction.

We see striking differences between the relative amplitudes of various peaks in the two projections. In the  $a$  projection, the first image of the ridge ( $\sim 6$  mrad) is stronger relative to the central ridge than it is in the  $c$  projection, while the second image ( $\sim 13$  mrad) is weaker. Note that both curves in Fig. 2 are based on similarly (area) normalized 2D-ACAR distributions, permitting us to make absolute comparisons of the sort considered here. The differences between the magnitude of the anisotropies are not unexpected and are often observed when different projection directions are compared. Also, the results of this paragraph are found to be insensitive to the precise functions  $S(p)$  used to obtain the anisotropic distributions through Eq. (1).

We have examined various sections (not shown) through the  $a$  projection of Fig. 1 as a function of  $p_y$  to assess possible changes in the ridge width for different  $p_z$  values;  $p_z$  values in the first as well as higher umklapp zones were investigated. This is an interesting question because  $c$ -axis dispersion of the bands, whose importance has been emphasized recently,<sup>14</sup> should manifest itself as changes in the ridge width as a function of  $p_z$ , possible complications introduced by the momentum dependence of the matrix elements notwithstanding. Although some changes in the width and shape of the ridge are seen, we found it difficult to establish an obvious substantial effect within experimental resolution. No clear FS crossings in the sections along the  $c$  direction were found either for a variety of  $p_y$  values. A more extensive analysis of the data is required to establish the detailed  $c$ -axis dispersion of bands and/or possible FS crossings along the  $c$  axis.

### III. CONCLUSIONS

We have presented the  $a$ -axis-projected 2D-ACAR data from an *untwinned* single crystal of  $\text{YBa}_2\text{Cu}_3\text{O}_{6.9}$

and shown that there is consistency between measured projections in the  $a$  and  $c$  directions. The structure in the data is dominated by the Cu-O chains and the associated ridge Fermi surface extending along the  $\Gamma Z$  direction, and the related umklapp images at higher momenta. The present results—when combined with the previously reported  $c$  projected 2D-ACAR spectra—allow us to deduce that the ridge FS is an approximately flat surface parallel to the  $\Gamma X$ - $\Gamma Z$  plane, consistent with the corresponding band-theory predictions;<sup>22–24</sup> within the experimental resolution, no firm conclusions concerning the  $c$ -axis dispersion of bands are drawn, although progress in this regard may be possible by further analysis of the data. Direct comparisons between the measured and theoretically predicted 2D-ACAR's, of the sort that have already proven crucially valuable in interpreting and explaining the  $c$ -projected 2D-ACAR's in  $\text{YBa}_2\text{Cu}_3\text{O}_7$ ,<sup>15–20</sup> will be essential for understanding various characteristic spectral features (e.g., relative intensities of the various images of the ridge FS in the  $a$ - and the  $c$ -axis projections, the detailed  $c$ -axis dispersion, etc.), and for assessing the extent of validity of the band-theory-based framework in describing the  $a$ -projected data.

### ACKNOWLEDGMENTS

The authors want to thank R. Benedek, L. Hoffmann, A. Manuel, and M. Peter for valuable discussions. The present work was supported by the U. S. Department of Energy, Basic Energy Sciences, Division of Materials Sciences under contract No. W-31-109-ENG-38 (LS,YF,KB), including a subcontract to Northeastern University (AB), and the National Science Foundation's Office of Science and Technology Centers under contract No. STC-8809854 (UW). This work benefited from the allocation of supercomputer time on the NERSC and San Diego Supercomputer centers.

- <sup>1</sup>L. Hoffmann, A. A. Manuel, M. Peter, E. Walker, and M. A. Damento, *Europhys. Lett.* **6**, 61 (1988); L. Hoffmann, A. A. Manuel, M. Peter, E. Walker, and M. A. Damento, *Physica C* **153-155**, 129 (1988); M. Peter, *IBM J. Res. Dev.* **33**, 333 (1988); B. Barbiellini, P. Genoud, J. Y. Henry, L. Hoffmann, T. Jarlborg, A. A. Manuel, S. Massida, M. Peter, W. Sadowski, H. J. Scheel, A. Shukla, A. K. Singh, and E. Walker, *Phys. Rev. B* **43**, 7810 (1991).
- <sup>2</sup>L. C. Smedskjaer, J. Z. Liu, R. Benedek, D. G. Legnini, D. J. Lam, M. D. Stahulak, H. Claus, and A. Bansil, *Physica C* **156**, 269 (1988).
- <sup>3</sup>H. Haghghi, J. H. Kaiser, S. Rayner, R. N. West, M. J. Fluss, R. H. Howell, P. E. A. Turchi, A. L. Wachs, Y. C. Jean, and Z. Z. Wang, *J. Phys. Condens. Matter* **2**, 1911 (1990).
- <sup>4</sup>H. Haghghi, J. H. Kaiser, S. Rayner, R. N. West, J. Z. Liu, R. Shelton, R. H. Howell, F. Solar, and M. J. Fluss, *Phys. Rev. Lett.* **67**, 382 (1991); *J. Phys. Chem. Solids* **52**, 1535 (1991).
- <sup>5</sup>L. C. Smedskjaer, A. Bansil, U. Welp, Y. Fang, and K. G. Bailey, *J. Phys. Chem. Solids* **52**, 1541 (1991).
- <sup>6</sup>L. C. Smedskjaer, A. Bansil, U. Welp, Y. Fang, and K. G. Bailey, *Physica C* **192**, 259 (1992).
- <sup>7</sup>L. Hoffmann, W. Sadowski and M. Peter, (unpublished).
- <sup>8</sup>For a recent discussion see *J. Phys. Chem. Solids* (to be published).
- <sup>9</sup>P. E. Mijnders, A. F. J. Melis, A. W. Weber, A. A. Menovshy, and K. Kadowaki, *Physica C* **176**, 113 (1991).
- <sup>10</sup>L. P. Chan, D. R. Harshman, K. G. Lynn, S. Massida, and D. B. Mitzi, *Phys. Rev. Lett.* **67**, 1350 (1991).
- <sup>11</sup>S. Tanigawa, Y. Mizuhara, Y. Hidaka, M. Oda, M. Suzuki, and T. Murakami, *Mater. Res. Soc.* **5**, 57 (1988).
- <sup>12</sup>P. E. A. Turchi, A. L. Wachs, K. H. Wetzler, J. H. Kaiser, R. N. West, Y. C. Yean, R. H. Howell, and M. J. Fluss, *J. Phys. Cond. Matter.* **2**, 1635 (1990); R. H. Howell *et al.*, (unpublished).
- <sup>13</sup>L. Hoffmann *et al.* (private communications). Their results appear similar to our results.
- <sup>14</sup>P. W. Anderson (unpublished).
- <sup>15</sup>A. Bansil, R. Pankaluto, R. S. Rao, P. E. Mijnders, W. Dlugosz, R. Prasad, and L. C. Smedskjaer, *Phys. Rev. Lett.* **61**, 2480 (1988).
- <sup>16</sup>A. Bansil, P. E. Mijnders, and L. C. Smedskjaer, *Physica C* **172**, 175 (1990); A. Bansil, *J. Phys. Chem. Solids* **52**, 1493 (1991).
- <sup>17</sup>A. Bansil, P. E. Mijnders, and L. C. Smedskjaer, *Phys. Rev. B* **43**, 3667 (1991).
- <sup>18</sup>S. Massida, *Physica C* **169**, 137 (1990).

- <sup>19</sup>D. Singh, W. E. Pickett, E. C. von Stetten, and S. Berko, *Phys. Rev. B* **42**, 2696 (1990).
- <sup>20</sup>T. Jarlborg, B. Barbiellini, E. Boronski, P. Genoud, and M. Peter, *J. Phys. Chem. Solids* **52**, 1515 (1991).
- <sup>21</sup>L. C. Smedskjaer and D. G. Legnini, *Nucl. Instrum. Methods Phys. Res. A* **292**, 487 (1990).
- <sup>22</sup>J. Yu, S. Massidda, A. J. Freeman, and D. D. Koelling, *Phys. Lett. A* **122**, 203 (1987).
- <sup>23</sup>W. E. Pickett, R. E. Cohen, and H. Krakauer, *Phys. Rev. B* **42**, 8764 (1990).
- <sup>24</sup>C. O. Rodriguez, A. I. Lichtenstein, I. I. Mazin, O. Jepsen, O. K. Andersen, and M. Methfessel, *Phys. Rev. B* **42**, 2692 (1990).

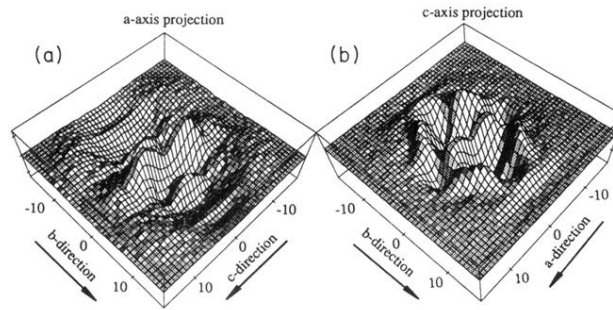


FIG. 1. A three-dimensional rendition of the *anisotropic* spectra  $A(\mathbf{p})$ , see Eq. (1), for untwinned  $\text{YBa}_2\text{Cu}_3\text{O}_{6.9}$ . (a) The present  $a$  projection, and (b) the  $c$  projection from the data of Ref. 5. The pixel size is  $0.8 \times 0.8 \text{ mrad}^2$ .